ISSN 0006-2979, Biochemistry (Moscow), 2018, Vol. 83, Nos. 12-13, pp. 1543-1551. © Pleiades Publishing, Ltd., 2018.
Originally published in Biochemistry (Moscow) On-Line Papers in Press, as Manuscript BM18-223, October 29, 2018.

Non-structural Functions of Hordeivirus Capsid Protein Identified in Plants Infected by a Chimeric Tobamovirus

S. S. Makarova[1], A. V. Makhotenko[1], A. V. Khromov[1], E. V. Skurat[1], A. G. Solovyev[2,3,a], V. V. Makarov[2], and N. O. Kalinina[2,b]*

[1]*Lomonosov Moscow State University, Biological Faculty, 119991 Moscow, Russia*
[2]*Belozersky Institute of Physico-Chemical Biology, Lomonosov Moscow State University, 119991 Moscow, Russia*
[3]*All-Russia Research Institute of Agricultural Biotechnology, 127550 Moscow, Russia*
[a]*e-mail: solovyev@belozersky.msu.ru*
[b]*e-mail: kalinina@genebee.msu.ru*

Received August 1, 2018
Revision received September 12, 2018

Abstract—Capsid proteins (CPs) of (+)RNA-containing plant viruses are multifunctional proteins involved in many stages of viral infection cycle, in addition to their main function of virus capsid formation. For example, the tobamoviral CP ensures virus systemic transport in plants and defines the virus–host interactions, thereby influencing the virus host range, virus infectivity, pathogenicity, and manifestation of infection symptoms. Hordeiviruses and tobamoviruses belong to the Virgaviridae family and have rod-shaped virions with a helical symmetry; their CPs are similar in structure. However, no non-structural functions of hordeiviral CPs have been described so far. In this study, we assayed possible non-structural functions of CP from the barley stripe mosaic virus (BSMV) (hordeivirus). To do this, the genome of turnip vein clearing virus (TVCV) (tobamovirus) was modified by substituting the *TVCV CP* gene with the *BSMV CP* gene or its mutants. We found that BSMV CP efficiently replaced TVCV CP at all stages of viral infection. In particular, BSMV CP performed the role of tobamoviral CP in the long-distance transport of the chimeric virus, acted as a hypersensitive response elicitor, and served as a pathogenicity determinant that influenced the symptoms of the viral infection. The chimeric tobamovirus coding for the *C*-terminally truncated BSMV CP displayed an increased infectivity and was transported in plants in a form of atypical virions (ribonucleoprotein complexes).

DOI: 10.1134/S000629791812012X

Keywords: plant viruses, chimeric tobamovirus, hordeivirus coat protein, transport, infection symptoms

Capsid proteins (CPs) of plant viruses encapsidate the viral genome, thereby protecting it from degradation. Although the assembly/disassembly of viral particles are canonical functions of CPs, in last decades, CPs have been recognized as multifunctional proteins involved in many stages of viral infection. CPs have different non-structural (not related to encapsidation) functions, such as regulation of viral replication, transcription, and translation [1-4].

Tobacco mosaic virus (TMV) CP is the most studied protein, both structurally and functionally, among CPs of helical plant viruses with (+)RNA genomes. Deletion of the tobamoviral CP gene affects cell-to-cell transport of ribonucleoprotein (RNP) complexes consisting of the virus-encoded movement protein (MP) and viral RNA [5]. Viral replication is less efficient in the absence of CP [6, 7]. Available experimental data suggest that TMV CP regulates, either directly or indirectly, formation of viral replication complexes, as well as synthesis and translation of subgenomic RNAs that, in turn, can influence formation of MP–RNA complexes and transport of the viral genome [7-10].

Other known TMV CP functions unrelated to encapsidation are pertinent to virus interaction with its host plant, in particular, to plant defense response. It was recently shown that TMV CP together with MP activate RNA degradation at the late infection stages resulting in

Abbreviations: BSMV, barley stripe mosaic virus; CD, circular dichroism; CP, coat protein (capsid protein); DLS, dynamic light scattering; HR, hypersensitive response; MP, movement protein; PMTV, potato mop-top virus; RNP, ribonucleoprotein complex; TGB proteins, movement proteins encoded by the triple gene block; TMV, tobacco mosaic virus; (wt)TVCV, (wild-type) turnip vein clearing virus.

* To whom correspondence should be addressed.

the inhibition of anti-viral systemic silencing [11]. TMV CP also elicits the hypersensitive response (HR) mediated by the *N′* resistance gene in *Nicotiana sylvestris* plants [12, 13]. CPs of other tobamoviruses are found to elicit HR mediated by different resistance genes in *Capsicum* species [14-16]. Besides, TMV CP can negatively regulate plant defense response by inducing suppression of defense-related signaling pathways [17, 18]. Mutation in TMV CP, such as amino acid substitutions or deletions and insertions of peptides, can considerably influence the symptoms and pattern of systemic infection in plants infected with mutant and chimeric viruses [12].

Hordeiviruses, as well as tobamoviruses, belong to the Virgaviridae family and represent (+)RNA plant viruses with the rod-shaped virions with helical symmetry [19]. Although tobamoviruses and hordeiviruses have structurally similar virions, they use different strategies of phloem transport resulting in systemic infection of the host plant. Unlike the tobamoviral CP, BSMV CP is not involved in the cell-to-cell movement and long-distance transport of the virus through the plant vascular system. Translocation of the BSMV genome in a form of RNP complexes at all stages of its transport is mediated by three MPs encoded by the triple gene block [20]. In hordeiviruses, two proteins play the role of pathogenicity determinants that determine viral virulence and infection symptoms: the silencing suppressor, small cysteine-rich protein essential for the virus long-distance transport [21], and viral replicase gamma-a subunit. It was also shown that the hordeiviral protein TGB1 elicits HR in barley [22].

Based on the structural similarity of BSMV and tobamoviral CPs [4] and previously reported infectivity of the TMV/BSMV chimeric construct representing the TMV genome (strain U1) in which the *TMV CP* gene was replaced with the *BSMV CP* gene [23], we created chimeric turnip vein clearing virus (TVCV, tobamovirus) that encoded BSMV CP or its mutants instead of its own CP. Using this experimental system, we studied the characteristics of chimeric virus infection in *Nicotiana benthamiana* in order to identify possible non-canonical functions of BSMV CP. BSMV CP functionally replaced tobamoviral CP without considerable decrease in the virus infectivity or ability for the long-distance transport. BSMV CP also acted as an HR elicitor and pathogenicity determinant and influenced the symptoms of viral infection.

MATERIALS AND METHODS

Recombinant constructs. Using the pQE30-BSMV-CP construct (earlier obtained in our laboratory) as a template, the *BSMV CP* gene was amplified with specific primers BSMV-CP-BamHI-P/BSMV-CP-M-SalI (table), digested with BamHI/SalI restriction endonucleases, and ligated into similarly digested construct representing the TVCV genome cloned in the pCambia1300 vector (http://www.cambia.org/daisy/cambia/585) by replacing the *TVCV CP* gene. Coding sequences for the deletion mutants ΔN-CP^{BSMV} and ΔC-CP^{BSMV} were amplified using pQE30-BSMV-CP as a template with specific primers BSMV-dN-P/BS-M-Bam and BSMV-CP-P-Xho/BSMV-dC-M, respectively (table). The resulting PCR products were digested with BamHI/XhoI and cloned into the pCambia1300 vector carrying a fragment of the TVCV genome.

Agrobacterium infiltration of *N. benthamiana* plants. *Nicotiana benthamiana* plants were grown from seeds and kept in controlled growth chambers with a 16/8 h day/night photoperiod at 25°C (day temperature) and 22°C (night temperature). *Agrobacterium tumefaciens* C58C1 cultures (kindly provided by Dr. J. Schiemann, Quedlinburg, Germany) containing binary vectors were

Primers used in the work

Name	Primer sequence (5'-3')
BSMV-CP-BamHI-P	GAGGATCCATGCCGAACGTTTCTTTGAC
BSMV-CP-M-SalI	TCGTCGACTCACGCTTCCTCGGCATC
BSMV-dN-P	AAACTCGAGATGGATTGGTGGGTCCACGTAGAAGC
BS-M-Bam	GCGGATCCTCACGCTTCCTCGGCATCTG
BSMV-CP-P-Xho	GGCTCGAGATGCCGAACGTTTCTTTGACTG
BSMV-dC-M	AAAGGATCCTCACACTGGGAGTCTCGCACTCT
TVCV-specific primer	ATCAGCAATGTCCACATCCA
F-BOX-P	GGCACTCACAAACGTCTATTTC
F-BOX-M	ACCTGGGAGGCATCCTGCTTAT
TVCV RdRp-P	CTCGGAGTCGCTAAAACCAG
TVCV RdRp-M	GAACGGAGCATCATTTTGTAAGC

grown to the exponential phase in Luria–Bertani medium (5 g/liter NaCl, 5 g/liter yeast extract, 10 g/liter tryptone) containing antibiotics, 20 μM acetosyringone, and 10 mM MES (Sigma, USA) in a shaker-incubator ES-20 (BioSan, Lithuania) at 190 rpm for 15-17 h at 28°C. *Agrobacterium tumefaciens* cells were collected by centrifugation (MiniSpin; Eppendorf, Germany) for 5 min at room temperature at 3000 rpm. The pellet was resuspended in 10 mM MES containing 10 mM $MgCl_2$ and 150 mM acetosyringone and incubated for 3 h at room temperature. For infiltration, the bacterial culture was diluted to an optical density OD_{600} = 0.2-0.4. The abaxial surfaces of two leaves in the lower leaf tier of 4-week-old plants were infiltrated with *A. tumefaciens* cell suspension using a needleless syringe.

Diaminobenzidine (DAB) staining. Plant leaves were placed in a DAB (Sigma) solution (1 mg/ml, pH 3.0) and then transferred to a desiccator; the vacuum was applied for 5 min. The leaves were incubated in the DAB solution on a shaker (BioSan) at 80-100 rpm for 4-5 h, then transferred to the bleaching solution (ethanol/acetic acid/glycerol, 3 : 1 : 1) and incubated until chlorophyll was completely removed.

Real-time PCR. RNA was extracted from plants using ExtractRNA reagent as recommended by the manufacturer (Evrogen, Russia). RNA concentration was measured spectrophotometrically. cDNA was synthesized with an MMVL RT kit (Evrogen) using either oligo-dT primer or TVCV-specific primer (table). The relative levels of viral RNA were determined by real-time PCR with the Quant Studio 3 Real-Time PCR System (Thermo Fisher Scientific, USA) using the qPCRmix-HS master mix (Evrogen). The F-box mRNA amplified with the primers F-BOX-P and F-BOX-M (table) was used for normalization of the TVCV RNA amplified with the primers TVCV RdRp-P and TVCV RdRp-M (table). Relative RNA content was estimated using the ΔC_t method according to the formula $2^{-\Delta Ct}$. The values are presented as mean ± standard deviation of three independent experiments. The data were analyzed using the Student's *t*-test; the significance level was assumed to be 0.01.

Western blotting. Leaf samples were ground with a pestle and mortar in liquid nitrogen, resuspended in gel loading buffer (2% SDS, 0.06 M Tris-HCl, pH 6.8, 0.001% bromophenol blue, 5% β-mercaptoethanol, 30% glycerol) (Sigma), and heated at 95°C for 5 min. The samples were fractionated by SDS-PAGE. Proteins were transferred from the gel to a nitrocellulose membrane with a pore size of 0.45 μm (Protran BA 85; GE Healthcare, USA). The membrane was incubated in 0.05 M Tris-HCl buffer, pH 7.2-7.4, with 5% dry milk (Sigma) and 0.05% Tween 20 (Serva, Germany) and stained with rabbit antibodies against BSMV CP (dilution, 1 : 10,000) and then with secondary goat anti-rabbit antibodies conjugated with horseradish peroxidase (dilution of 1 : 10,000; Sigma). The blots were developed using the ECL kit (GE Healthcare).

Virus isolation from infected plant leaves. Systemically infected plant leaves exhibiting specific symptoms of viral infection were collected at day 21 post infection. The leaves were ground with a pestle and mortar in liquid nitrogen with the addition of 0.3 M glycine-KOH buffer, pH 7.5, at the 1 : 3 (w/v) ratio. The extract was filtered to remove cell debris and centrifuged at 12,000 rpm for 30 min at 4°C (Beckman J-21 centrifuge; Beckman, USA). Triton X-100 (Sigma) was added to the supernatant to a final concentration of 1% (v/v), followed by 20-min incubation. Then, polyethylene glycol 6000 (Sigma) was added to a final concentration of 2.5% (w/w), and NaCl was added to a final concentration of 5% (w/w). The samples were incubated at 4°C overnight and centrifuged at 10,000 rpm for 20 min at 4°C (Beckman J-21). The pellet was resuspended in 0.025 M Tris-HCl buffer (pH 7.5); the suspension was clarified by centrifugation at 10,000 rpm for 15 min at 4°C and the resulting virus preparation was used for further characterization.

CD spectra of viral preparations were recorded in 1-mm cells at room temperature in a Chirascan CD spectrometer (Applied Photophysics, UK) in 5 mM phosphate buffer (pH 7.5) in the far-UV region (190-260 nm) at a rate of 0.5-1.0 nm/s with baseline subtraction. The recorded spectra were processed using a standard software package provided with the instrument. The CD spectra in the figure represent averages of several independent experiments. For each studied virus, at least three independent samples were analyzed.

Surface zeta potential and dynamic light scattering (DLS). Determination of the hydrodynamic diameter and measurement of the surface zeta potential were carried out with a Zetasizer Nano ZS (Malvern Instruments Ltd., UK) equipped with a He-Ne laser (633 nm, 10 mV). The temperature of the samples was maintained within 0.1°C using a Peltier temperature control system. Light scattering was measured at an angle of 173°. The autocorrelation functions were detected and processed with the Dispersion Technology Software (DTS) version 5.10 (Malvern Panalytical, UK). Polystyrene cuvettes with an optical path length of 10 mm were used for the measurements; the volume of the sample in a cuvette was 1 ml.

Preparation of ultrathin sections of *N. benthamiana* leaf mesophyll cells. A small fragment of systemically infected *N. benthamiana* leaf was washed in 100 mM phosphate buffer (pH 7.4) containing 2% sucrose. The fragment was cut into strips 1 mm thick and 2 mm long with a blade. The strips were placed in 2.5% glutaraldehyde solution (Sigma) in 100 mM phosphate buffer with 2% sucrose for 2.5-3 h, then washed with water, and transferred to 2% aqueous solution of osmium tetroxide for 2 h. Next, the samples were washed with water and sequentially dehydrated in 50% ethanol, 70% ethanol with 2% uranyl acetate (Polysciences, USA) (overnight,

to enhance contrast), 80%, 96% ethanol, and acetone. The samples were sequentially incubated in the acetone/Epon mixture (3 : 1) for 2 h, acetone/Epon mixture (1 : 1) for 1 h, acetone/Epon mixture (1 : 3) for 2 h, and Epon for 24 h. Next, the samples were incubated at 37°C for 24 h and then at 60°C for 48 h for Epon polymerization. Ultrathin sections (~100 nm) were cut with an LKB ultratome (Bromma, Sweden), stained with Reynolds reagent [24], and analyzed under a JEM-1400 electron microscope (JEOL, Japan).

RESULTS

Characteristics of *N. benthamiana* infection with the chimeric virus TVCV(CP^{BSMV}). Chimeric TVCV(CP^{BSMV}) construct was generated by replacement with the *BSMV CP* gene of the *TVCV CP* gene in the infectious TVCV cDNA cloned in the binary pCambia vector (http://www.cambia.org/daisy/cambia/585). *Nicotiana benthamiana* plants were infiltrated with *A. tumefaciens* carrying the TVCV(CP^{BSMV}) construct. Plants infiltrated with the agrobacterial culture carrying the wild-type TVCV construct (wtTVCV) were used as a control.

wtTVCV caused mild symptoms first appearing on the upper, systemically infected (non-infiltrated) leaves on the 10th day post infiltration (dpi). Later, the growth of infected plants was suppressed, and a strong deformation of upper leaves was observed (Fig. 1). Plants infected with the chimeric TVCV(CP^{BSMV}) virus developed the symptoms of infection with a slight delay: deformation of leaves associated with formation of small chlorotic regions and leaf crinkling was observed at 13 dpi (Fig. 1). Infiltrated leaves exhibited only a light curling. As a negative control, we used infectious TVCV cDNA clone in which the *TVCV CP* gene was replaced by the *GFP* gene. In *N. benthamiana* plants agroinfiltrated with this construct, GFP fluorescence was observed only in the infiltrated leaves, whereas the upper leaves exhibited no GFP fluorescence and symptoms of infection up to 21 dpi (data not shown).

The results of estimation of TVCV RNA accumulation in upper plant leaves by real-time PCR and Western blot analysis of BSMV CP were in a good agreement with the appearance of symptoms of infection (Figs. 2a and 2b). In TVCV(CP^{BSMV})-infected plants, BSMV CP was detected at 4 dpi in agroinfiltrated leaves and at 9 dpi in systemically infected leaves (Fig. 2a). Accumulation of TVCV(CP^{BSMV}) was approximately 2 times lower compared to the plants infected with wtTVCV in both agroinfiltrated leaves at 4 dpi and upper leaves at 14 dpi (Figs. 2b and 2c). These data demonstrate that in plants infected with the chimeric tobamovirus, the hordeiviral CP fulfilled the functions of the tobamoviral CP essential for the virus long-distance transport in plants, although hordeiviral CP it is not required for hordeivirus long-distance transport in *N. benthamiana*.

Properties of plant infection with chimeric virus mutants. For more detailed analysis of BSMV CP role in infection, we introduced mutations into the *BSMV CP* gene in the chimeric virus genome. The *N*- and *C*-terminal fragments of BSMV CP and TMV CP are known to be intrinsically disordered (i.e., lacking unique secondary or tertiary structures under physiological conditions) and exposed at the virion surface [4, 23, 25]. According to the current views, these disordered regions can play a major role in the encapsidation-unrelated functions of plant virus CPs due to their ability to interact with viral and cell factors [3, 26].

Using TVCV(CP^{BSMV}), we generated two viral constructs, namely the TVCV(ΔN-CP^{BSMV}) mutant encoding BSMV CP with deleted 30 *N*-terminal amino acid residues and the TVCV(ΔC-CP^{BSMV}) mutant encoding the BSMV CP with deleted 22 *C*-terminal amino acid residues. After *N. benthamiana* plants were infiltrated by agrobacteria carrying these constructs, the symptoms of

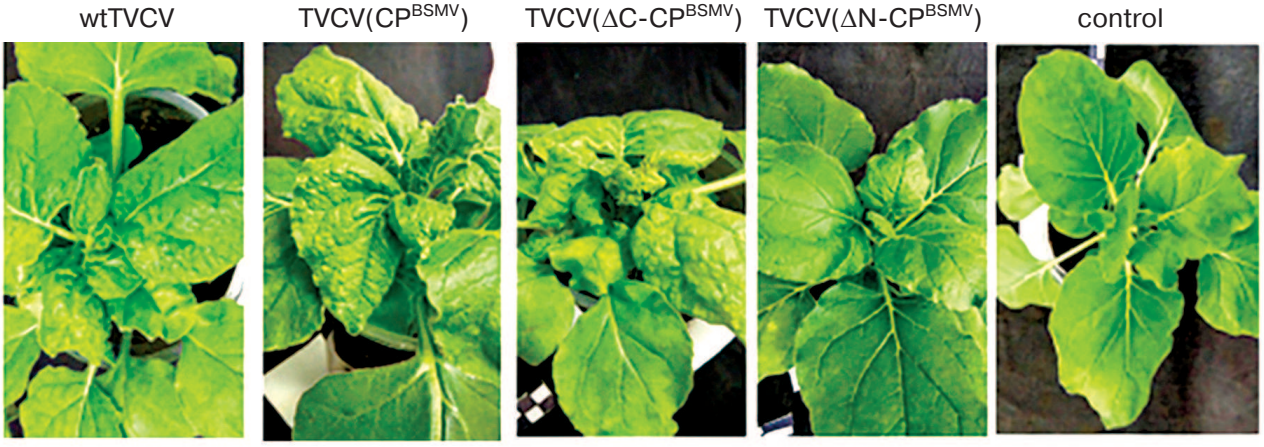

Fig. 1. Symptoms of viral infection observed at 14 dpi in *N. benthamiana* plants infected with chimeric virus TVCV(CP^{BSMV}) and chimeric viruses TVCV(ΔN-CP^{BSMV}) and TVCV(ΔC-CP^{BSMV}) carrying BSMV CP with deleted N- and C-terminal regions, respectively. Non-infected plants were used as a control.

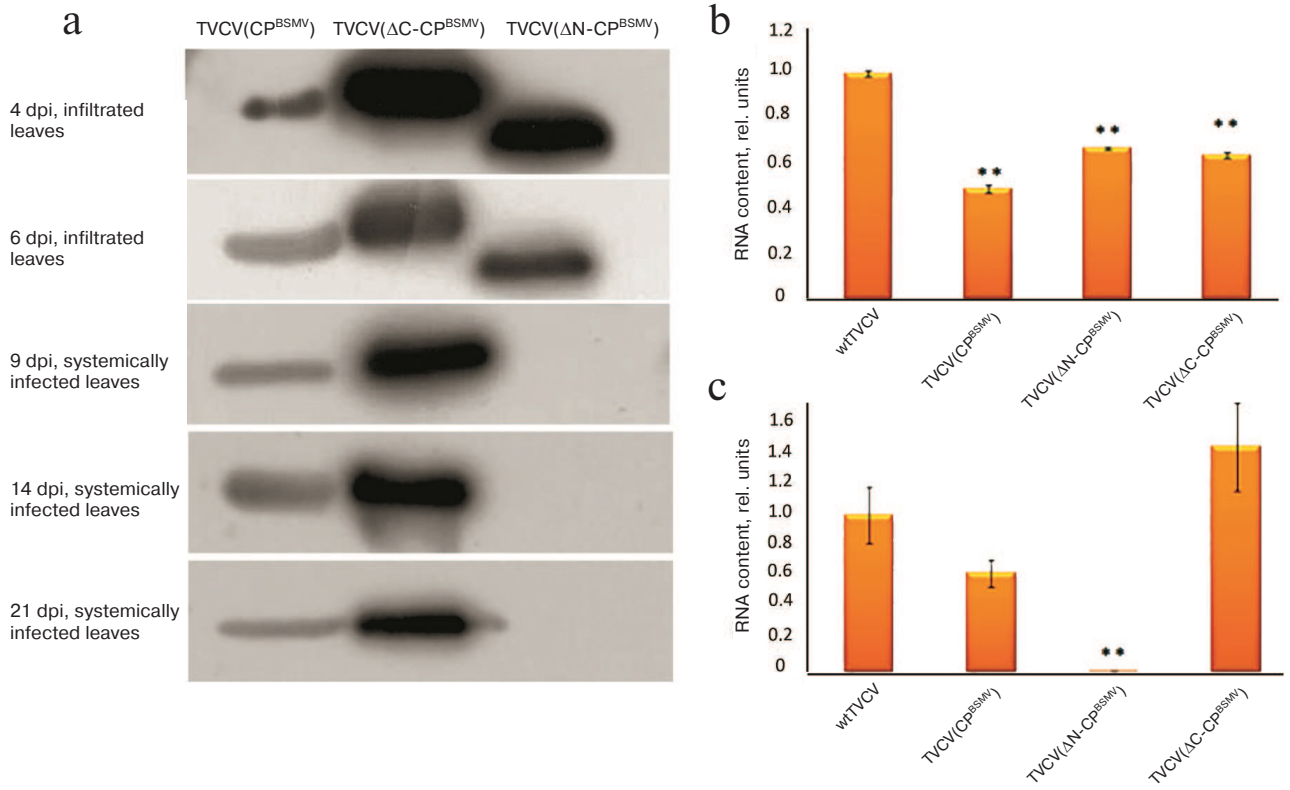

Fig. 2. Detection of BSMV CP and TVCV RNA at different time points in agroinfiltrated and systemically infected upper leaves of *N. benthamiana* plants infected by chimeric viruses TVCV(CP^{BSMV}), TVCV(ΔN-CP^{BSMV}), and TVCV(ΔC-CP^{BSMV}). a) Western blot analysis of BSMV CP accumulation in plants infected by the chimeric virus TVCV(CP^{BSMV}) and its mutants TVCV(ΔN-CP^{BSMV}) and TVCV(ΔC-CP^{BSMV}) at 4 and 6 dpi in agroinfiltrated leaves and at 9, 14, and 21 dpi in systemically infected leaves. Analysis of TVCV RNA accumulation by real-time PCR in infected leaves of *N. benthamiana* at (b) 7 dpi and (c) in systematically infected leaves at 14 dpi. **, indicates statistically significant difference in the TVCV RNA levels with plants infected with wtTVCV ($p < 0.01$).

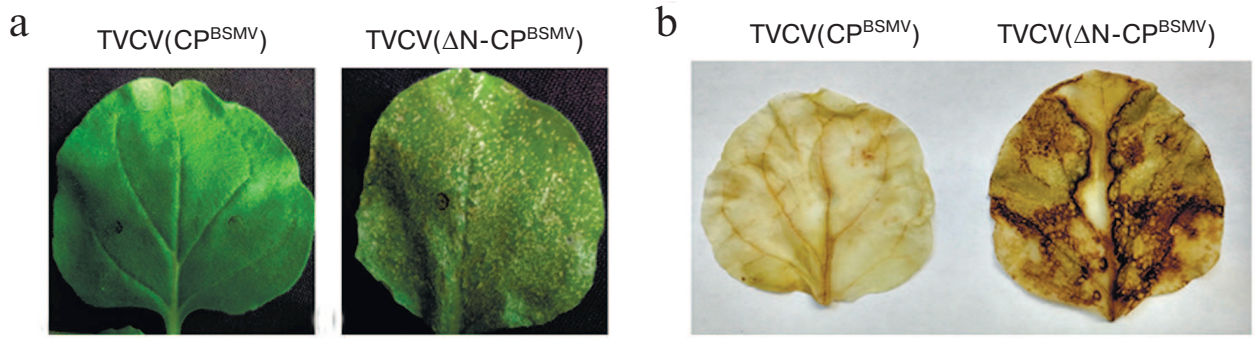

Fig. 3. Symptoms of virus infection in plants infected with TVCV(ΔN-CP^{BSMV}). a) Necrotic lesions on agroinfiltrated leaves at 6 dpi. b) DAB staining for reactive oxygen species of leaves infected with TVCV(CP^{BSMV}) and TVCV(ΔN-CP^{BSMV}) at 4 dpi.

infection on the upper non-infiltrated leaves of plants infected with TVCV(ΔC-CP^{BSMV}) appeared at 10 dpi, i.e., 3 days earlier than the same symptoms in the case of TVCV(CP^{BSMV}) infection (13 dpi). Interestingly, the symptoms in plants infected with TVCV(ΔC-CP^{BSMV}) and wtTVCV appeared simultaneously. At 14 dpi, the infection was fully manifested as rosette tops, general dwarfism, and occasional cases of chlorosis (Fig. 1). Local necroses typical for HR were observed on leaves agroinfiltrated with TVCV(ΔN-CP^{BSMV}) at 6 dpi (Fig. 3a), whereas no symptoms of infection on upper non-inoculated leaves were found (Fig. 1).

Real-time PCR analysis of TVCV RNA content in agroinfiltrated leaves at 7 dpi and systemically infected

leaves at 14 dpi revealed higher levels of TVCV(ΔC-CP^{BSMV}) RNA compared to TVCV(CP^{BSMV}) (Figs. 2b and 2c). These data were confirmed by Western blotting with antibodies against BSMV CP: at all times analyzed, the amount of BSMV ΔC-CP was considerably higher than the amount of BSMV CP (Fig. 2a). In the case of TVCV(ΔN-CP^{BSMV}) infection, both TVCV RNA and BSMV CP were detected only in the agroinfiltrated leaved, but not in the upper leaves (Fig. 2, a-c).

To identify the nature of necrosis induced by TVCV(ΔN-CP^{BSMV}) (Fig. 3a), agroinfiltrated leaves were stained with diaminobenzidine (DAB) at 4 dpi, i.e., at the time point when no necrotic lesions have formed yet. DAB is routinely used for *in situ* detection of reactive oxygen species in plants, since it is oxidized by hydrogen peroxide with the formation of dark brown precipitate [27, 28]. DAB staining of leaves agroinfiltrated with the TVCV(ΔN-CP^{BSMV}) construct, but not with TVCV(CP^{BSMV}), resulted in their pronounced staining (Fig. 3b), therefore confirming that the observed necrosis was a result of HR, since the development of HR is known to be preceded by accumulation of reactive oxygen species in plant tissues [29].

Physico-chemical characteristics of mutant chimeric virus TVCV(ΔC-CP^{BSMV}). We also analyzed physico-chemical characteristics of the mutant chimeric TVCV(ΔC-CP^{BSMV}) virus that accumulated in agroinfiltrated and systemically infected leaves at higher levels than TVCV(CP^{BSMV}). Preparations of the chimeric virus and its mutant were isolated from infected leaves at 21 dpi.

The absorption spectrum of TVCV(ΔC-CP^{BSMV}) preparations had a pronounced maximum at 260 nm, showing the presence of a considerable portion (>5%) of nucleic acids (data not shown). The near-UV circular dichroism (CD) spectrum of TVCV(ΔC-CP^{BSMV}) was typical of helical plant viruses enriched with α-helical elements and displayed two negative maxima at 208 and 222 nm. Superposition of the CD spectra obtained for TVCV(ΔC-CP^{BSMV}) and TVCV(CP^{BSMV}) demonstrated their similarity (Fig. 4a) and pointed out the absence of considerable alterations in the CP secondary structure in virions formed by TVCV(ΔC-CP^{BSMV}).

The surface zeta potential of the viral particles (−28 mV) was similar to that of the wild-type TMV virions (−30 mV, data not shown) (Fig. 4b). Therefore, the *C*-terminal truncation of BSMV CP had no considerable influence on either protein structure or its surface properties.

On the other hand, measurements of the hydrodynamic parameters of the viral particles formed by BSMV ΔC-CP by the DLS method demonstrated the presence of two distinct peaks of 100 and 800 nm (Fig. 4c). This hydrodynamic pattern suggests that in solution the viral particles exist as large structures (aggregates). The hydrodynamic diameter of virions formed by the chimeric tobamovirus was ~35 nm (data not shown).

Analyses of TVCV(ΔC-CP^{BSMV}) preparations by transmission electron microscopy (TEM) demonstrated the presence of thread-like structures that were 10 nm thick, had irregular length (from 100 to several hundred nanometers) and low electron density, and formed net-like agglomerates (data not shown). Therefore, the TVCV(ΔC-CP^{BSMV}) structures considerably differed from BSMV rod-shaped virions. To characterize these structures, sections of leaves infected with TVCV(ΔC-CP^{BSMV}) and TVCV(CP^{BSMV}) were examined by TEM. Unlike virus particles of ~20 nm in diameter observed for the wild-type and chimeric tobamoviruses (Fig. 5a) [23], TVCV(ΔC-CP^{BSMV}) formed 10 nm-thick flexible, often aggregated particles. The presence of such particles not only in purified preparations, but also in plant cells sug-

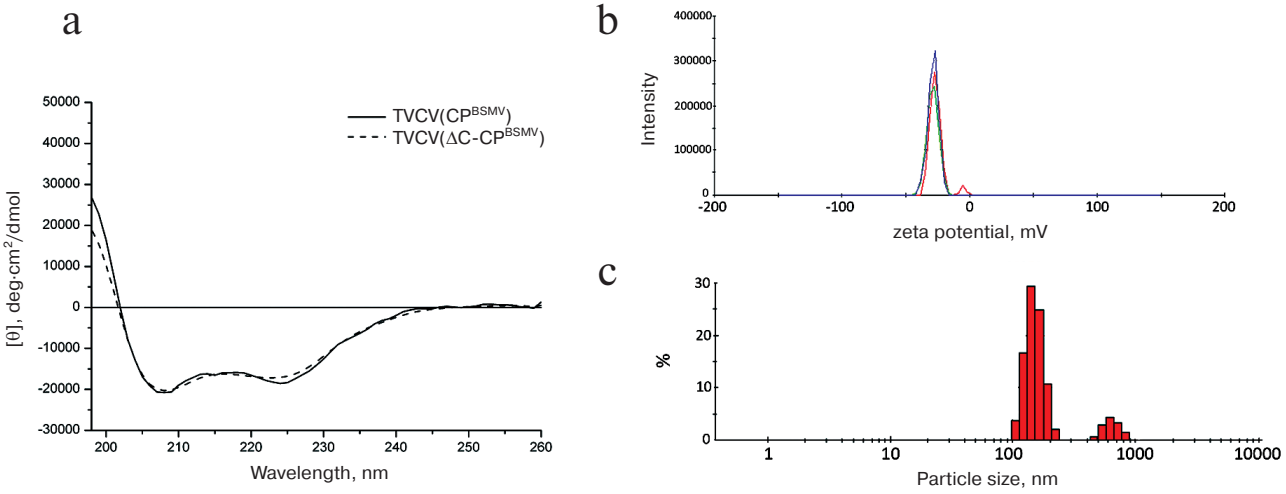

Fig. 4. Physico-chemical characteristics of the chimeric TVCV(ΔC-CP^{BSMV}) virus. a) CD spectra of TVCV(CP^{BSMV}) and TVCV(ΔC-CP^{BSMV}) preparations. b) Surface zeta potential of TVCV(ΔC-CP^{BSMV}) virus particles. Three independent measurements are shown in different colors. c) Hydrodynamic diameter of TVCV(ΔC-CP^{BSMV}) particles determined by the DLS method.

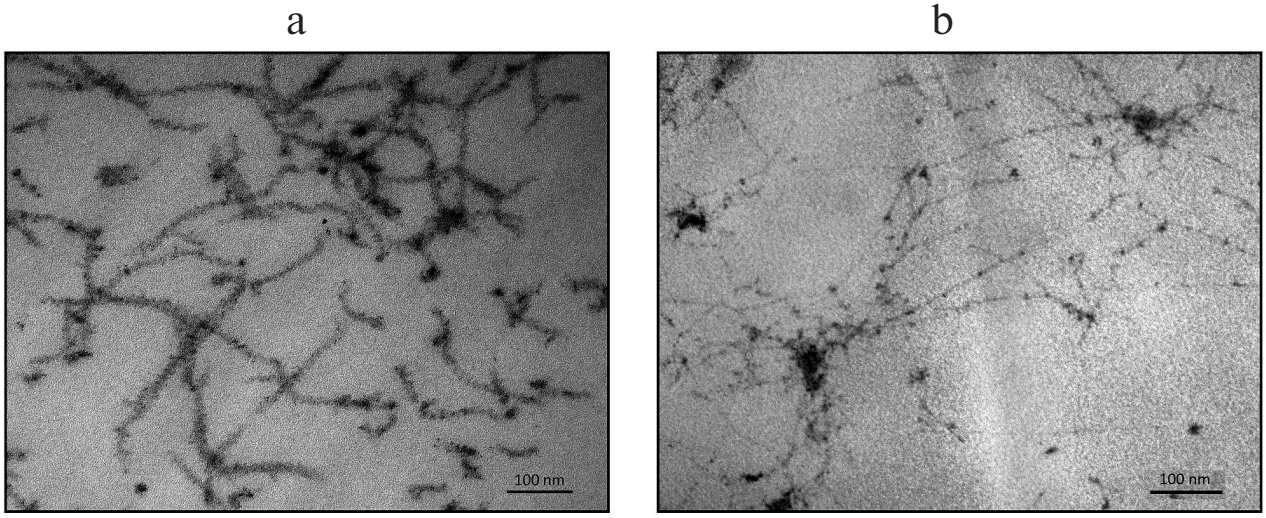

Fig. 5. Electron microscopy of sections of systemically infected *N. benthamiana* leaves exhibiting symptoms of viral infection. Plants were infected with (a) TVCV(CP^{BSMV}) and (b) TVCV(ΔC-CP^{BSMV}).

gests that their abnormal appearance is an inherent feature rather than an artifact.

DISCUSSION

Here, we demonstrated that the *BSMV CP* gene can replace the *CP* gene in the TVCV genome without significant losses in the virus infectivity and ability for long-distance transport. This finding was rather unexpected since it is known that the hordeiviral CP is not required for the phloem transport of BSMV [19-21]. However, the results of our work prove that BMSV CP can nevertheless provide this function in the context of the recombinant viral genome. This functional switch from virion to non-virion transported form of the viral genome resembles the role of CP in the long-distance transport in the case of potato mop-top virus (PMTV, genus *Pomovirus*) closely related to hordeiviruses. Genomic RNA3 of PMTV is transported through the phloem as a modified virion, whereas RNA1 and RNA2 are transported in a form of RNP complexes [30].

As previously demonstrated, the infection phenotype and the host range of hordeiviruses are affected by the interactions of several nonstructural viral proteins, such as gamma-a (RNA replicase subunit), gamma-b (silencing suppressor and systemic transport factor), and the transport TGB1 protein encoded by the triple gene block [19, 22]. It is believed that these viral proteins influence genome replication, regulation of viral gene expression, and/or virus translocation, either directly or indirectly. On the other hand, during tobamovirus infection the majority of these functions are associated with the viral CP. For example, tobamoviral CP participates in the virus phloem transport [30] and plays a dual role in the regulation of the host plant defense response, on one hand, by acting as an elicitor of HR [12-16, 31, 32] and on another hand, by participating in suppression of plant defense systems [11, 17, 18].

The ability of BSMV CP to effectively perform the functions of tobamoviral CP in the chimeric tobamovirus can have two different complementary explanations. The main role of tobamoviral CP is encapsidation of viral RNA genome and its protection during the phloem transport. Indeed, mutations in the TMV genomic RNA region responsible for the initiation of virion assembly not only block formation of viral particles, but also suppress long-distance transport of the virus [9]. It was shown that when encapsidated by the full-length BSMV CP, chimeric TMV tobamovirus can form morphologically correct virions indistinguishable from the wild-type BSMV virions thereby efficiently protecting tobamoviral RNA from degradation [23]. Another explanation is based on the fact that CP has other than structural functions. TMV CP is necessary for entrance of viral genome into the phloem. It was found that mutant TMV lacking the CP gene could only reach the vascular parenchyma cells in minor leaf veins and was not detected in companion cells involved in the virus entry into the phloem sieve elements [10]. Efficient replacement of the tobamoviral CP by the hordeiviral CP is likely due to the structural similarity of these proteins most pronounced in the region of the core α-helices [4]. This structural similarity may also explain the involvement of BSMV CP in the regulation of plant defense response manifested as HR in the case of BSMV CP mutant with deleted intrinsically disordered *N*-terminal region. Indeed, it has been demonstrated that the region responsible for the TMV CP activity as an elicitor of HR is located in the area of core α-helices

exposed at the virion surface [12]. We propose that structurally similar region in BSMV CP with deleted *N*-terminus becomes more accessible for the interacting factors in the chimeric tobamovirus, which results in the HR development. Similar effects were observed for deletion mutants of other plant viruses. For example, a *C*-terminal deletion in the TMV CP resulted in the induction of HR in *A. thaliana* [33], whereas deletion of the *N*-terminal fragment in the CP of the bacilliform/isometric brome mosaic virus led to the HR development in infected *Chenopodium quinoa* plants [35].

The fact that deletion of 22 amino acid residues forming a fragment of intrinsically disordered *C*-terminal region of the BSMV CP results in considerable increase in the chimeric virus infectivity is rather unexpected. The increase in infectivity is manifested as earlier appearance of infection symptoms on the upper plant leaves as well as elevated levels of mutant CP and viral RNA in agroinfiltrated and systemically infected leaves in comparison to the chimeric virus with the full-length CP. Characterization of viral preparations isolated from the infected plants demonstrated that deletion of BSMV CP *C*-terminal fragment did not noticeably affect protein structure (as determined by CD spectrometry) and surface properties (as determined by measuring zeta potential) in comparison to the wild type BSMV CP. However, in solution, these particles formed high-molecular-weight aggregates. Electron microscopy of the infected cell sections revealed that these particles were abnormally thin (10 nm), whereas the diameter of viral particles of the wild-type and chimeric tobamoviruses was ~20 nm. Intrinsically disordered *C*-terminal region is not involved in the formation of intersubunit interaction in mature virions [23]. However, we cannot exclude that this protein region is involved into initiation or early stages of virion assembly; therefore, the absence of the *C*-terminal region can result in the formation of aberrant virions (RNP complexes). In general, the characteristics of aberrant particles (morphology and measured parameters) were similar to those of filamentous helical viruses and a presumable non-virion transport form of viral genome such as RNP complexes formed by viral movement proteins and virus RNA *in vitro* (parameters, tendency to form aggregates) [36-38]. Our data show the importance of the CP *C*-terminal region for correct virion assembly. At the same time, the aberrant virions demonstrated high efficiency of systemic transport of chimeric viral RNA in a form of RNP complexes, while the mutant BSMV CP was capable of providing all necessary CP functions in the cell-to-cell (short-distance) transport and long-distance phloem types of viral transport. In addition, the *C*-terminal part of CP molecule is likely recognized by the plant defense system, and therefore, its deletion can result in virus ability to partially escape defense responses of host plants. The experimental system developed in this work can be used for further studies of various strategies of systemic transport used by rod-shaped plant viruses and elucidation of fundamental mechanisms of plant defense.

Funding

This work was supported by the Russian Science Foundation (project no. 14-24-0007, obtaining of genetic constructs, plant infection and experimental analysis, physico-chemical characterization of viral proteins). The work of A. G. Solovyev was supported by the Russian Foundation for Basic Research (grant no. 15-04-03922, bioinformatics analysis).

Authors' Contributions

N. O. Kalinina and V. V. Makarov planned the experiments, discussed results, and wrote the manuscript. S. S. Makarova generated genetic constructs and performed all main experiments with virus-infected plants. A. V. Makhotenko and A. V. Khromov performed real-time PCR. A. G. Solovyev and E. V. Skurat designed mutations of the chimeric virus and took part in discussions.

Acknowledgements

The authors are grateful to S. Yu. Kurchashova for her help in preparing sections of infected leaves and A. N. Prusov for his assistance in electron microscopy imaging.

Conflicts of Interest

The authors declare no conflicts of interest.

REFERENCES

1. Ni, P., and Kao, C. C. (2013) Non-encapsidation activities of the capsid proteins of positive-strand RNA viruses, *Virology*, **446**, 123-132.
2. Weber, P. H., and Bujarski, J. J. (2015) Multiple functions of capsid proteins in (+) stranded RNA viruses during plant–virus interactions, *Virus Res.*, **22**, 140-149.
3. Makarov, V. V., and Kalinina, N. O. (2016) Structure and noncanonical activities of capsid proteins of helical plant viruses, *Biochemistry (Moscow)*, **81**, 1-18.
4. Solovyev, A. G., and Makarov, V. V. (2016) Helical capsids of plant viruses: architecture with structural lability, *J. Gen. Virol.*, **97**, 1739-1754.
5. Carrington, J. C., Kasschau, K. D., Mahajan, S. K., and Schaad, M. C. (1996) Cell-to-cell and long-distance transport of viruses in plants, *Plant Cell*, **8**, 1669-1681.
6. Ryabov, E. V., Robinson, D. J., and Taliansky, M. E. (1999) A plant virus-encoded protein facilitates long-distance movement of heterologous viral RNA, *Proc. Natl. Acad. Sci. USA*, **96**, 1212-1217.

7. Bendahmane, M., Szecsi, J., Chen, I., Berg, R. H., and Beachy, R. N. (2002) Characterization of mutant tobacco mosaic virus capsid protein that interferes with virus cell-to-cell movement, *Proc. Natl. Acad. Sci. USA*, **99**, 3645-3650.
8. Asurmendi, S., Berg, R. H., Koo, J. C., and Beachy, R. N. (2004) Coat protein regulates formation of replication complexes during tobacco mosaic virus infection, *Proc. Natl. Acad. Sci. USA*, **101**, 1415-1420.
9. Saito, T., Yamanaka, K., and Okada, Y. (1990) Long distance movement and viral assembly of tobacco mosaic virus mutants, *Virology*, **176**, 329-336.
10. Ding, S. W., Li, W. X., and Symons, R. H. (1995) A novel naturally occurring hybrid gene encoded by a plant RNA virus facilitates long distance virus movement, *EMBO J.*, **14**, 5762-5772.
11. Conti, G., Zavallo, D., Venturuzzi, A. L., Rodriguez, M. C., Crespi, M., and Asurmendi, S. (2017) TMV induces RNA decay pathways to modulate gene silencing and disease symptoms, *Plant J.*, **89**, 73-84.
12. Culver, J. N. (2002) Tobacco mosaic virus assembly and disassembly: determinants in pathogenicity and resistance, *Annu. Rev. Phytopathol.*, **40**, 287-308.
13. Taraporewala, Z. F., and Culver, J. N. (1997) Structural and functional conservation of the tobamovirus capsid protein elicitor active site, *Mol. Plant Microbe Interact.*, **10**, 597-604.
14. Huh, S. U., Choi, L. M., Lee, G. J., Kim, Y. J., and Paek, K. H. (2012) Capsicum annuum WRKY transcription factor d (CaWRKYd) regulates hypersensitive response and defense response upon tobacco mosaic viral infection, *Plant Sci.*, **197**, 50-58.
15. Gilardi, P., Garcia-Luque, I., and Serra, M. T. (2004) The coat protein of tobamovirus acts as elicitor of both L2 and L4 gene-mediated resistance in *Capsicum*, *J. Gen. Virol.*, **85**, 2077-2085.
16. Berzal-Herranz, A., de la Cruz, A., Tenllado, F., Diaz-Ruiz, J. R., Lopez, L., Sanz, A. I., Vaquero, C., Serra, M. T., and Garcia-Luque, I. (1995) The *Capsicum* L3 gene-mediated resistance against the tobamoviruses is elicited by the coat protein, *Virology*, **209**, 498-505.
17. Conti, G., Rodriguez, M. C., Manacorda, C. A., and Asurmendi, S. (2012) Transgenic expression of tobacco mosaic virus capsid and movement proteins modulate plant basal defense and biotic stress responses in *Nicotiana tabacum*, *Mol. Plant Microbe Interact.*, **10**, 1370-1384.
18. Rodriguez, M., Conti, G., Zavallo, D., Manacorda, C., and Asurmendi, S. (2014) TMV Cg capsid protein stabilizes DELLA proteins and in turn negatively modulates salicylic acid-mediated defense pathway during *Arabidopsis thaliana* viral infection, *BMC Plant Biol.*, **14**, 210-216.
19. Jackson, A. O., Lim, H. S., Bragg, J., Ganesan, U., and Lee, M. Y. (2009) Hordeivirus replication, movement, and pathogenesis, *Annu. Rev. Phytopathol.*, **47**, 385-422.
20. Verchot-Lubicz, J., Torrance, L., Solovyev, A. G., Morozov, S. Y., Jackson, A. O., and Gilmer, D. (2010) Varied movement strategies employed by triple gene block-encoding viruses, *Mol. Plant Microbe Interact.*, **23**, 1231-1247.
21. Hipper, C., Brault, V., Ziegler-Graff, V., and Revers, F. (2013) Viral and cellular factors involved in phloem transport of plant viruses, *Front. Plant Sci.*, **4**, 154.
22. Lee, M. Y., Yan, L., Gorter, F. A., Kim, B. Y., Cui, Y., Hu, Y., Yuan, C., Grindheim, J., Ganesan, U., Liu, Z., Han, C., Yu, J., Li, D., and Jackson, A. O. (2012) *Brachypodium distachyon* line Bd3-1 resistance is elicited by the barley stripe mosaic virus triple gene block 1 movement protein, *J. Gen. Virol.*, **93**, 2729-2739.
23. Clare, D. K., Pechnikova, E. V., Skurat, E. V., Makarov, V. V., Sokolova, O. S., Solovyev, A. G., and Orlova, E. V. (2015) Novel inter-subunit c contacts in barley stripe mosaic virus revealed by cryo-electron microscopy, *Structure*, **23**, 1815-1826.
24. Edward, S., and Reynolds, E. S. (1963) The use of lead citrate at high pH as an electron-opaque stain in electron microscopy, *J. Cell Biol.*, **17**, 208-212.
25. Makarov, V. V., Skurat, E. V., Semenyuk, P. I., Abashkin, D. A., Kalinina, N. O., Arutyunyan, A. M., Solovyev, A. G., and Dobrov, E. N. (2013) Structural lability of barley stripe mosaic virus virions, *PLoS One*, **8**, e60942.
26. Xue, B., Blocquel, D., Habchi, J., Uversky, A. V., Kurgan, L., Uversky, V. N., and Longhi, S. (2014) Structural disorder in viral proteins, *Chem. Rev.*, **114**, 6880-6911.
27. Daudi, A., and O'Brien, J. (2012) Detection of hydrogen peroxide by DAB staining in *Arabidopsis* leaves, *Bio. Protoc.*, **2**, e263.
28. Mehdy, M. C. (1994) Active oxygen species in plant defense against pathogens, *Plant Physiol.*, **105**, 467-472.
29. Conti, G., Rodriguez, M. C., Manacorda, C. A., and Asurmendi, S. (2012) Transgenic expression of tobacco mosaic virus capsid and movement proteins modulate plant basal defense and biotic stress responses in *Nicotiana tabacum*, *Mol. Plant Microbe Interact.*, **10**, 1370-1384.
30. Solovyev, A. G., and Savenkov, E. I. (2014) Factors involved in the systemic transport of plant RNA viruses: the emerging role of the nucleus, *J. Exp. Bot.*, **65**, 1689-1697.
31. Conti, G., Rodriguez, M. C., Venturuzzi, A. L., and Asurmendi, S. (2017) Modulation of host plant immunity by tobamovirus proteins, *Ann. Bot.*, **119**, 737-747.
32. Culver, J. N., Stubbs, G., and Dawson, W. O. (1994) Structure–function relationship between tobacco mosaic virus coat protein and hypersensitivity in *Nicotiana sylvestris*, *J. Mol. Biol.*, **242**, 130-138.
33. Kurihara, Y., and Watanabe, Y. A. (2004) TMV-Cg mutant with a truncated coat protein induces cell death resembling the hypersensitive response in *Arabidopsis*, *Mol. Cells.*, **17**, 334-339.
34. Li, M., Li, P., Song, R., and Xu, Z. (2010) An induced hypersensitive-like response limits expression of foreign peptides via a recombinant TMV-based vector in a susceptible tobacco, *PLoS One*, **5**, e15087.
35. Rao, A. L., and Grantham, G. L. (1995) Biological significance of the seven amino-terminal basic residues of brome mosaic virus coat protein, *Virology*, **211**, 42-52.
36. Kim, S. H., MacFarlane, S., Kalinina, N. O., Rakitina, D. V., Ryabov, E. V., Gillespie, T., Haupt, S., Brown, J. W., and Taliansky, M. (2007) Interaction of a plant virus-encoded protein with the major nucleolar protein fibrillarin is required for systemic virus infection, *Proc. Natl. Acad. Sci. USA*, **104**, 11115-11120.
37. Makarov, V. V., Makarova, S. S., Makhotenko, A. V., Obraztsova, E. A., and Kalinina, N. O. (2015) *In vitro* properties of hordeivirus TGB1 protein forming ribonucleoprotein complexes, *J. Gen. Virol.*, **96**, 3422-3431.
38. Kiselyova, O. I., Yaminsky, I. V., Karger, E. M., Frolova, O. Y., Dorokhov, Y. L., and Atabekov, J. G. (2001) Visualization by atomic force microscopy of tobacco mosaic virus movement protein–RNA complexes formed *in vitro*, *J. Gen. Virol.*, **82**, 1503-1508.